Baselga Moreno, S.; García-Asenjo Villamayor, L.; Garrigues Talens, P. (2015). Deformation monitoring and the maximum number of stable points method. Measurement. 70:27-35. doi:10.1016/j.measurement.2015.03.034.

Deformation monitoring and the maximum number of stable points method

S. Baselga[a], L. García-Asenjo[b] and P. Garrigues[c]

[a](Corresponding author) Cartographic Engineering, Geodesy and Photogrammetry Dpt., Universidad Politécnica de Valencia, Camino de Vera s/n, 46022 Valencia, Spain. Tel: +34 963877000 ext. 75556 E-mail: serbamo@cgf.upv.es

[b]Cartographic Engineering, Geodesy and Photogrammetry Dpt., Universidad Politécnica de Valencia, Camino de Vera s/n, 46022 Valencia, Spain. Tel: +34 963877000 ext. 75512 E-mail: lugarcia@cgf.upv.es

[c]Cartographic Engineering, Geodesy and Photogrammetry Dpt., Universidad Politécnica de Valencia, Camino de Vera s/n, 46022 Valencia, Spain. Tel: +34 963877000 ext. 75558 E-mail: pasgarta@cgf.upv.es

Abstract. The question of determination of displacements in control networks with two or more measuring epochs is a well-known problem with broad applications to different fields of science and engineering. The standard procedure, which is computed by means of the pseudoinverse matrix, however, makes an implicit assumption that may be not convenient for the network at hand: it distributes the noticed displacement among the majority of the network points. The present paper develops what it has been named as the maximum number of stable points hypothesis and builds from the corresponding theoretical framework an applicable computation procedure. Application to a particular example will confirm its clear advantages versus the standard procedure for deformation determination in the cases where a single large deformation may be suspected.

Keywords: deformation monitoring, least squares, robust estimation, global optimization, surveying, distance measurement

1. Introduction

The theory and methods for deformation determination can be found in disparate areas of science and engineering, which include structural engineering, geodesy, surveying engineering, tectonics, geotechnical engineering and geomorphology, and may make use of observation techniques like Global Navigation Satellite Systems (GNSS) – e.g. Global Positioning System (GPS) – remote sensing, photogrammetry, Electronic Distance Measurement (EDM), angle measuring, levelling, etc. [1-10].

Control networks for deformation determination are generally classified into absolute and relative networks, depending whether they have points located outside the deformable area that can be considered stable (absolute networks) or all the network points may be affected by displacements so that only relative movements can be detected (relative networks) [7]. In the present paper, we will focus on the latter case, i.e. the case where all points are potential candidates for suffering a displacement between a pair of observing epochs.

In a deformation network redundant measurements are made among the control points for every epoch. Then the corresponding overdetermined systems of observing equations are formed and solved by least squares. Finally, the use of statistical tests over the least squares solution permits to conclude within the corresponding level of significance on the possible point displacements. This well-known theoretical framework will be developed in the next section. As it will be shown, no unique solution exists for the problem of determining relative displacements. In fact there are infinitely many solutions in terms of possible point displacements that are compatible with the observed values. In order to obtain a solution for the corresponding rank deficient systems the standard theory of deformation determination opts then for the pseudoinverse solution. As it will be

argued, the pseudoinverse solution is a very sensible choice but it may not be the best option for all cases. The fact that the particular selected solution supposes to include an additional assumption directly affecting the results and what this assumption may be is a question often overlooked in deformation monitoring theory. The explanation of the assumption implicit in the adoption of the pseudoinverse solution (balanced distribution of displacements among all points) along with the proposal of a different assumption and correspondingly different solution arguably more sensible for other cases (stability of the majority of pillars and possible large displacements in very few of them) will be developed in the next section and later applied to the case of the open test field located in the *Universidad Politécnica de Valencia* campus.

2. Methods

2.1. Standard procedure for deformation determination

Let the system of observation equations for epoch 1 be written as

$$A_1 x_1 = l_1 + r_1 \tag{1}$$

where A_1 denotes the coefficient matrix, x_1 the solution vector, l_1 the vector of independent terms, which includes the observed values, and r_1 the residual vector.

If observations are assumed to follow normal distributions with variance-covariance matrix Σ_1 then the residual vector also follows a normal distribution with zero mean and variance-covariance matrix Σ_1 and the most likely solution is obtained by the least squares condition $\arg\min_{x_1} r_1^T P_1 r_1$, where $P_1 = \Sigma_1^{-1}$, which leads to

$$\left(A_1^T P_1 A_1\right) x_1 = A_1^T P_1 l_1 \tag{2}$$

$$x_1 = \left(A_1^T P_1 A_1\right)^{-1} A_1^T P_1 l_1 \tag{3}$$

and analogously for epoch 2

$$x_2 = \left(A_2^T P_2 A_2\right)^{-1} A_2^T P_2 l_2 \tag{4}$$

The deformation vector is obtained then as

$$d = x_2 - x_1 \tag{5}$$

If the magnitudes observed in both epochs are the same (and ordered the same in both equation systems) and the same approximate coordinates are used in both epochs, Eq. (1) applied to both epochs can be written as

$$A x_1 = l_1 + r_1 \tag{6}$$

$$A x_2 = l_2 + r_2 \tag{7}$$

Subtracting Eq. (6) from Eq. (7) it can be written

$$A d = l + r \tag{8}$$

where *d* is the deformation vector defined in Eq. (5), *l* is vector of differences between observed values in every epoch and *r* is the vector of differences between residuals.

Solution of the equation system in Eq. (8), named the observation differences model, is obviously equivalent to the separate solution of Eqs. (6) and (7) and subsequent determination of displacement by Eq. (5), and it will be preferred here for the sake of conciseness. The least squares solution verifies

$$\left(A^T PA\right)d = A^T Pl \tag{9}$$

$$d = \left(A^T PA\right)^{-1} A^T Pl \tag{10}$$

where $P = \left(\Sigma_1 + \Sigma_2\right)^{-1}$.

Now, as it was mentioned before, in the case of control networks where no point is free from potential displacements the corresponding system of equations is rank deficient. Therefore the matrix inverse in Eq. (10) – or inverses in Eqs. (3) and (4) if separate adjustments are preferred – does not exist. The solution is obtained then by means of generalized inverses, denoted by $(\cdot)^-$, in an equivalent manner

$$d = \left(A^T PA\right)^- A^T Pl \tag{11}$$

where, by definition, given a matrix $B \in \Re^{m\times n}$ a generalized inverse of *B* is a matrix $B^- \in \Re^{n\times m}$ that satisfies

$$BB^-B = B \tag{12}$$

The question now is that there are infinitely many generalized inverses, leading each of them to a different solution. There are then infinitely many deformation solutions that fulfill the least squares minimum condition, or in other words, there are infinitely many vectors *d* that satisfy Eq. (8) with the same residual vector *r*.

One particular generalized inverse is customarily selected: the pseudoinverse matrix. For any given matrix $B \in \Re^{m\times n}$ there always exists one and only one matrix – denoted by B^+ – that satisfies the four equations known as Moore-Penrose conditions [11]

$$BB^+B = B \tag{13}$$

$$B^+BB^+ = B^+ \tag{14}$$

$$\left(BB^+\right)^T = BB^+ \tag{15}$$

$$\left(B^+B\right)^T = B^+B \tag{16}$$

The pseudoinverse matrix is one of the generalized inverse matrices and it can be proved that has some *possibly* desirable properties that make it the habitual choice [12,13]: it is the generalized inverse of least determinant and least trace, and provides the solution of minimum L_2-norm among the infinitely many solutions of the system of equations.

The crucial point here is to acknowledge the assumption implicit in the customary selection of the pseudoinverse for the generalized inverse matrix in Eq. (11): the displacement vector *d* with least L_2-norm is being chosen as the best explicative solution to our rank deficient problem. In other words, in a control network where no point can be assured to remain stable we opt for the solution where Σd_i^2 is minimum, i.e. we prefer to explain the observed differences between epochs in the measured magnitudes as *small displacements of all points*, and this constitutes a working

assumption incapable of being demonstrated or refuted (additional to those that led to select the least squares estimator as the best estimator).

One may argue that this hypothesis may appear to be reasonable for most cases. There are some occasions, however, where this assumption may go against the expected behavior, and therefore the customary use of the pseudoinverse solution must clearly be avoided. This is the case, for instance, of highly stable networks, such as the test field facility that we will see in Section 3, where clearly no displacements of the order of the observation accuracy may be expected, except for the possible displacement of one of the benchmarks due to unfortunate circumstances. Explanation of the deformation sensed by the measurements as multiple displacements of all points – which is the solution obtained by means of the pseudoinverse – would be clearly unacceptable and a different assumption and corresponding solution is needed.

2.2. Maximum number of stable points procedure

Rather than postulating as the best explicative solution the one that extends the displacement to all points (making them as small as possible) the assumption of isolating the displacements in as few points as possible may be occasionally preferred. We will refer to this assumption as the maximum number of stable points assumption. Operationally, we will obtain this by searching among the infinitely many solutions *d* of Eq. (11) for the one that minimizes L_1-norm, i.e. $\Sigma|d_i|$ minimum. This property of the L_1-norm versus the behavior of the L_2-norm is well-known and has been extensively used in the domain of the residual vector in what is known as robust estimation: the ability of the least L_1-norm estimator ($\Sigma|r_i|$ minimum) to confine large values in the residuals of the very few affected observations versus the behavior of the least L_2-norm estimator (Σr_i^2 minimum) that results in not so large values but spread out throughout all results [14-17]. Now this ability will be exploited in the deformation space.

Considering that all solutions (and only them) of the rank-deficient system of consistent equations $Bx = b$ where $B \in \Re^{m \times n}$ and $b \in \Re^m$ verify

$$x = B^+ b + \left(I - B^+ B\right) y \tag{17}$$

for $y \in \Re^n$ and B^+ pseudoinverse of B (e.g., [11]), the solution of the rank-deficient least squares system given in Eq. (9) can also be obtained by

$$d = \left(A^T PA\right)^+ A^T Pl + \left(I - \left(A^T PA\right)^+ \left(A^T PA\right)\right) y \tag{18}$$

Assigning the value $y = 0$ leads to the pseudoinverse solution

$$d = \left(A^T PA\right)^+ A^T Pl \tag{19}$$

which, as it can be demonstrated (see Appendix), is the solution of least L_2-norm (Σd_i^2 minimum).

However, as we are now interested in the solution of least L_1-norm ($\Sigma|d_i|$ minimum) we will seek for the *y*-vector in Eq. (18) that minimizes this norm. In Robust Estimation the search for the minimum L_1-norm is normally done following an Iteratively Reweighted Least Squares (IRLS) scheme [1,14]. Nevertheless, if the minimization is dealt with as a Global Optimization (GO) problem it is ensured that the optimum attained is not only a local minimum but the global one, which sometimes results in a very significant improvement with respect to the result obtained by the IRLS method [14,17]. The optimization problem to solve is

$$\begin{cases} \min\limits_{y} \sum\limits_{i=1}^{n} |d_i| \\ \text{where } d = \left(A^T PA\right)^{+} A^T Pl + \left(I - \left(A^T PA\right)^{+} \left(A^T PA\right)\right) y \\ \text{for } y \in \Re^n \end{cases} \tag{20}$$

Among all the GO methods we can select, for instance, the Simulated Annealing (SA) method. Random values will be iteratively drawn for the *y*-vector, plugged into Eq. (20) and the subsequent L_1-norm values stored. The role of the SA algorithm is to put some order into this process of random search so that it finally results into the global optimum. For details on the method the reader is referred, e.g., to [14,18]. It must be noted that the solution of the GO problem stated in Eq. (20) may also be successfully obtained by any other of the existing GO methods, to name just a few: Genetic Algorithms [19,20], Interval Arithmetic Techniques [21], Monkey Algorithms [22,23], hybrid methods [23], etc.

2.3. Statistical testing of displacements

Independently of the generalized inverse matrix selected one has to finally test whether the determined displacements are significant (at a certain level of significance) or not. The so-called Global Congruency Test, e.g. [7,25], is routinely applied in order to investigate the hypotheses of zero displacement, which constitutes the null hypothesis

$$H_0 : d = 0 \tag{21}$$

and significant displacement, which is the alternative hypothesis

$$H_1 : d \neq 0 \tag{22}$$

It is performed by means of the statistic

$$T = \frac{d^T \left(A^T PA\right) d}{\sigma_0{}^2 h} \tag{23}$$

where

$$\sigma_0{}^2 = \frac{r^T Pr}{m - h} \tag{24}$$

is the unit weight variance (with *m* the number of observations) and *h* is the rank of $A^T PA$.

Comparison between the *T* value obtained and the critical value at a level of significance α for the corresponding Fisher distribution permits to decide between the two possible alternatives: if $T < F(h, m-h, 1-\alpha)$ then the null hypothesis (no significant displacement) is accepted, if $T > F(h, m-h, 1-\alpha)$ then the alternative hypothesis (significant displacement) is accepted.

The test can also be done in 1D, i.e. particularized to a single coordinate of the network, to decide on its possible significant displacement; or 2D to test the possible displacement of a point. In those

cases only the components of interest of the *d*-vector and the corresponding minor of the matrix $A^T PA$ have to be used along with $h = 1$ (1D-case) or $h = 2$ (2D-case).

3. Application and results

Let us now present an example of application where the hypothesis of the maximum number of stable points is more convenient than the standard assumption defined by the use of the pseudoinverse solution and let us analyse how they both perform for the same simulated displacements.

A test field has been recently set at the *Universidad Politécnica de Valencia* campus and its corresponding absolute scale has been transferred from the Nummela baseline [26] by means of an observation campaign with a Mekometer ME5000 EDM, previously calibrated by interferometric means. The expected baseline stability has now to be confirmed. Fig. 1 displays the baseline geometry, which is basically intended for calibration of EDMs and, therefore, is of the so-called Heerbrugg-type design [27].

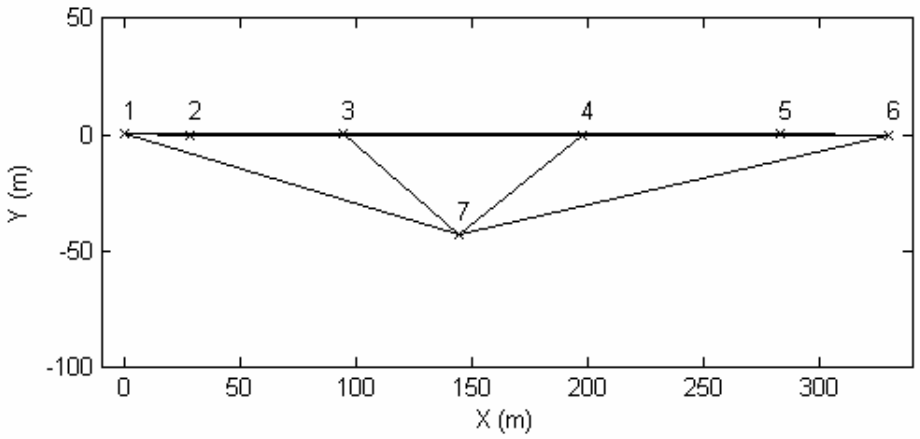

Fig. 1. UPV test field (local coordinates).

Apart from the epoch zero data (scale transfer from Nummela with the calibrated EDM) where coordinates were obtained for the baseline pillars with absolute accuracies of 0.2 to 0.3 mm, let us now suppose that we perform a second observation campaign with a simulated displacement in one pillar, possibly due to unfortunate circumstances, of an amount that, in principle, could be clearly detectable after distance measurement with accuracies of few tenths of a millimetre: say a displacement of 1 mm.

Therefore, we will compare the distance values deduced from the epoch zero coordinates, which constitute our first campaign, with the distance values deduced from the epoch zero coordinates plus the simulated coordinate displacement, which constitute our second campaign. The additional inclusion of randomly simulated observation errors – of the few tenths of a millimeter expected for the Mekometer ME5000 – show to have a second order impact on the obtained results and therefore do not obscure the essential issues of the discussion below.

Tables 1 to 6 and corresponding Figs. 2 to 7 show the solutions obtained by both procedures – pseudoinverse solution and the maximum number of stable points procedure – for the respective simulated displacements of 1 mm in X_1, Y_1, X_2, Y_2, X_7, Y_7. For the purpose of illustration only those cases are shown. Results for simulated displacements in pillars 3, 4, 5 and 6 are similar to those obtained for pillars 1 and 2. Additionally, please also note that the unknowns to determine

also include, as usual, the possible calibration coefficients *a* and *b* that relate distances measured in the second campaign to absolute distances traced to the meter definition measured in the first campaign, $D_2 = (1+a)D_1 + b$.

Table 1. Results for a simulated displacement of 1 mm in X_1.

Unknown	Pseudoinverse	Min L_1-norm
a (ppm)	1,6	0,2
b (mm)	0,00	0,00
dX_1 (mm)	0,60	0,95
dY_1 (mm)	0,00	0,00
dX_2 (mm)	-0,35	-0,04
dY_2 (mm)	0,00	0,00
dX_3 (mm)	-0,24	-0,03
dY_3 (mm)	0,01	0,00
dX_4 (mm)	-0,07	-0,02
dY_4 (mm)	0,01	0,00
dX_5 (mm)	0,07	0,00
dY_5 (mm)	0,02	0,00
dX_6 (mm)	0,14	0,01
dY_6 (mm)	0,02	0,00
dX_7 (mm)	-0,16	-0,02
dY_7 (mm)	-0,06	-0,01

Fig. 2. Results for a simulated displacement dX_1 = 1 mm. Dotted/solid bars represent the pseudoinverse/min L_1-norm solution. Units: mm except for unknown *a* given in ppm.

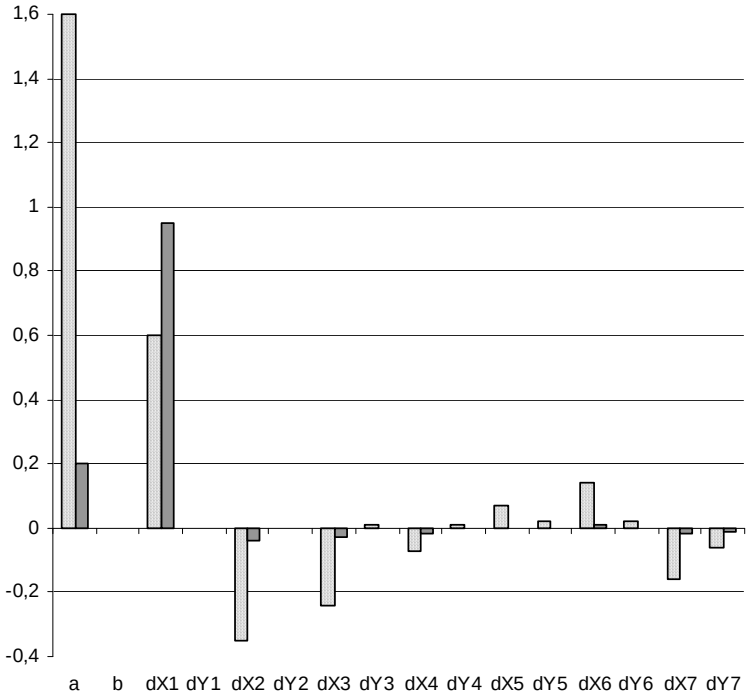

Table 2. Results for a simulated displacement of 1 mm in Y_1.

Unknown	Pseudoinverse	Min L_1-norm
a (ppm)	-0,1	0,0
b (mm)	0,00	0,00
dX_1 (mm)	0,00	0,00
dY_1 (mm)	0,61	0,93
dX_2 (mm)	0,00	0,00
dY_2 (mm)	-0,35	-0,07
dX_3 (mm)	-0,01	0,00
dY_3 (mm)	-0,24	-0,05
dX_4 (mm)	-0,01	0,00
dY_4 (mm)	-0,07	-0,02
dX_5 (mm)	-0,02	0,00
dY_5 (mm)	0,07	0,00
dX_6 (mm)	-0,02	0,00
dY_6 (mm)	0,14	0,01
dX_7 (mm)	0,06	0,01
dY_7 (mm)	-0,16	-0,04

Fig. 3. Results for a simulated displacement dY_1 = 1 mm. Dotted/solid bars represent the pseudoinverse/min L_1-norm solution. Units: mm except for unknown *a* given in ppm.

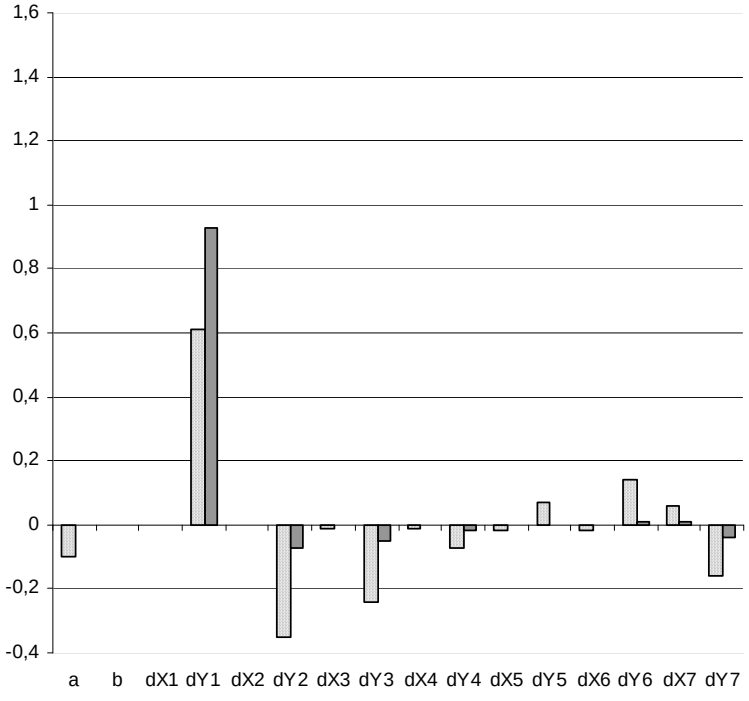

Table 3. Results for a simulated displacement of 1 mm in X_2.

Unknown	Pseudoinverse	Min L_1-norm
a (ppm)	1,3	0,2
b (mm)	0,00	0,00
dX_1 (mm)	-0,35	-0,04
dY_1 (mm)	0,00	0,00
dX_2 (mm)	0,69	0,96
dY_2 (mm)	0,00	0,00
dX_3 (mm)	-0,22	-0,03
dY_3 (mm)	0,00	0,00
dX_4 (mm)	-0,08	-0,01
dY_4 (mm)	0,01	0,00
dX_5 (mm)	0,03	0,00
dY_5 (mm)	0,02	0,00
dX_6 (mm)	0,09	0,01
dY_6 (mm)	0,02	0,00
dX_7 (mm)	-0,15	-0,02
dY_7 (mm)	-0,05	-0,01

Fig. 4. Results for a simulated displacement dX_2 = 1 mm. Dotted/solid bars represent the pseudoinverse/min L_1-norm solution. Units: mm except for unknown *a* given in ppm.

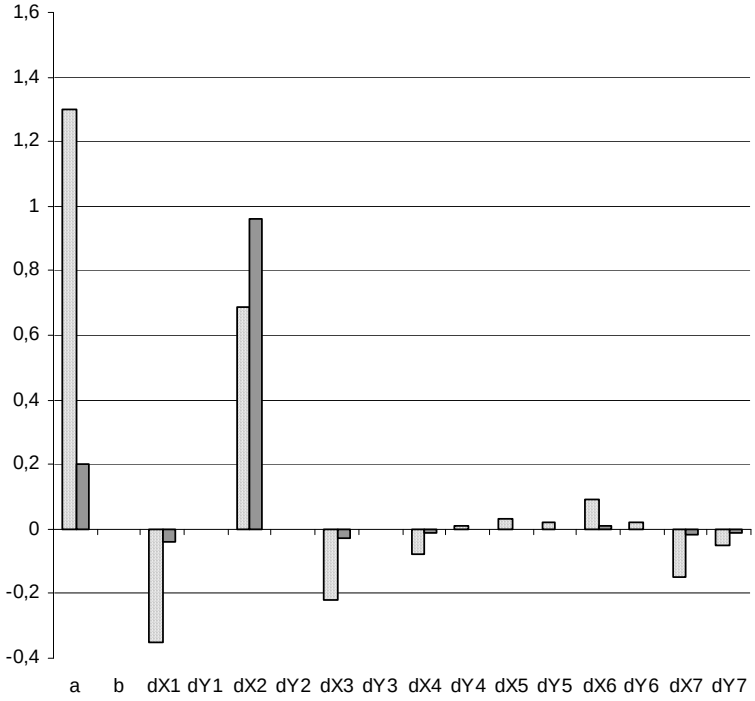

Table 4. Results for a simulated displacement of 1 mm in Y_2.

Unknown	Pseudoinverse	Min L_1-norm
a (ppm)	-0,1	0,0
b (mm)	0,00	0,00
dX_1 (mm)	0,00	0,00
dY_1 (mm)	-0,35	-0,05
dX_2 (mm)	0,00	0,00
dY_2 (mm)	0,69	0,95
dX_3 (mm)	0,00	0,00
dY_3 (mm)	-0,22	-0,04
dX_4 (mm)	-0,01	0,00
dY_4 (mm)	-0,08	-0,01
dX_5 (mm)	-0,02	0,00
dY_5 (mm)	0,03	0,00
dX_6 (mm)	-0,02	0,00
dY_6 (mm)	0,09	0,01
dX_7 (mm)	0,05	0,01
dY_7 (mm)	-0,15	-0,03

Fig. 5. Results for a simulated displacement dY_2 = 1 mm. Dotted/solid bars represent the pseudoinverse/min L_1-norm solution. Units: mm except for unknown *a* given in ppm.

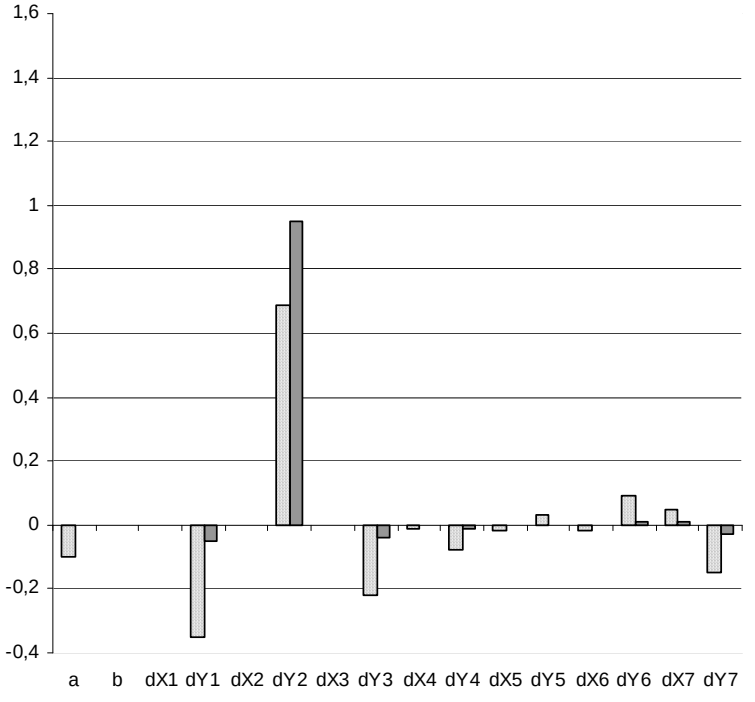

Table 5. Results for a simulated displacement of 1 mm in X_7.

Unknown	Pseudoinverse	Min L_1-norm
a (ppm)	0,1	0,1
b (mm)	0,00	0,00
dX_1 (mm)	-0,16	-0,02
dY_1 (mm)	0,06	0,00
dX_2 (mm)	-0,15	-0,02
dY_2 (mm)	0,05	0,00
dX_3 (mm)	-0,15	-0,02
dY_3 (mm)	0,02	0,00
dX_4 (mm)	-0,14	-0,01
dY_4 (mm)	-0,02	0,00
dX_5 (mm)	-0,13	0,00
dY_5 (mm)	-0,05	0,00
dX_6 (mm)	-0,12	0,00
dY_6 (mm)	-0,07	0,00
dX_7 (mm)	0,84	0,99
dY_7 (mm)	0,00	0,00

Fig. 6. Results for a simulated displacement dX_7 = 1 mm. Dotted/solid bars represent the pseudoinverse/min L_1-norm solution. Units: mm except for unknown *a* given in ppm.

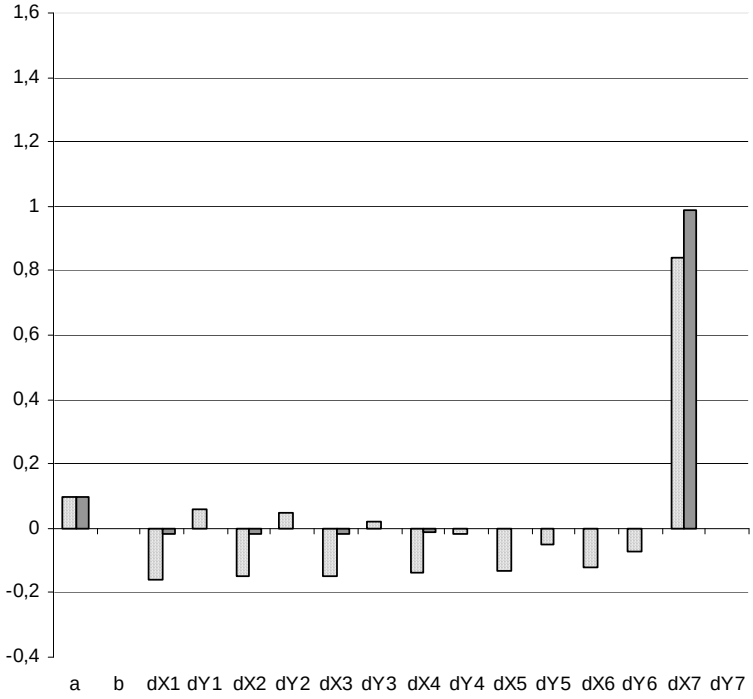

Table 6. Results for a simulated displacement of 1 mm in Y_7.

Unknown	Pseudoinverse	Min L_1-norm
a (ppm)	0,4	0,0
b (mm)	0,00	0,00
dX_1 (mm)	-0,06	0,00
dY_1 (mm)	-0,16	-0,01
dX_2 (mm)	-0,05	0,00
dY_2 (mm)	-0,15	-0,01
dX_3 (mm)	-0,02	0,00
dY_3 (mm)	-0,15	-0,01
dX_4 (mm)	0,02	0,00
dY_4 (mm)	-0,14	-0,01
dX_5 (mm)	0,05	0,00
dY_5 (mm)	-0,13	-0,01
dX_6 (mm)	0,07	0,00
dY_6 (mm)	-0,12	-0,01
dX_7 (mm)	0,00	0,00
dY_7 (mm)	0,84	0,99

Fig. 7. Results for a simulated displacement dY_7 = 1 mm. Dotted/solid bars represent the pseudoinverse/min L_1-norm solution. Units: mm except for unknown *a* given in ppm.

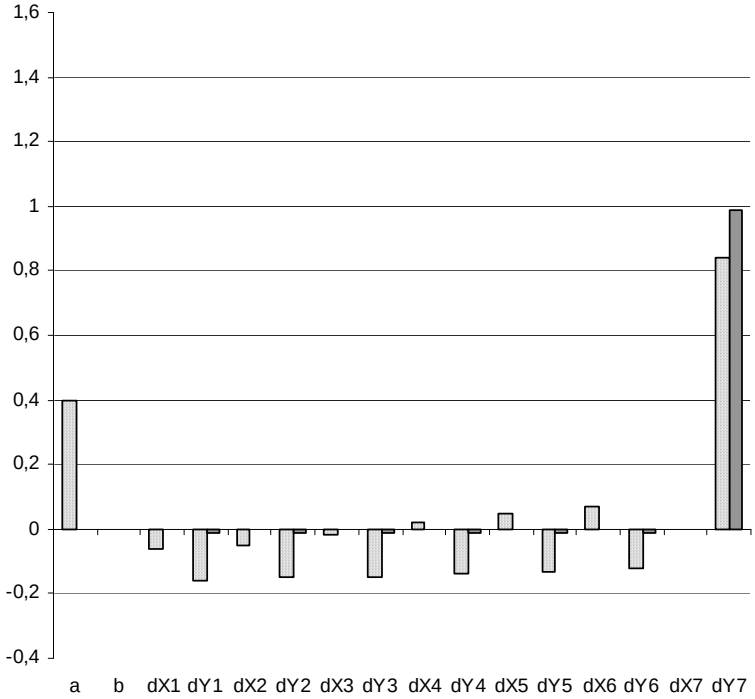

As we see, the standard procedure for deformation determination (based on the pseudoinverse solution) notices the deformation suffered by the network but fails clearly in determining where this displacement occurred. This is due to the fact, explained in Section 2.1, that the standard determination procedure prefers to assign displacements to the majority of the pillars (the majority of unknowns, in general) of the network. The assumption of a single large displacement in a pillar versus the assumption of many not so large displacements but affecting most of the pillars may sometimes, as in this example, be more convenient and the corresponding theoretical framework shall be applied. The results obtained after the standard pseudoinverse lead to a misleading scene in which many of the presumably stable pillars have suffered significant displacements. It is particularly remarkable how a simulated displacement in pillar No. 1 can be misleadingly interpreted as a change of scale *a* of the distancemeter by the standard method due to the existing correlations in the network. By contrast, the application of the maximum number of stable points procedure faithfully captures the simulated single displacement and assigns only residual values to the rest of the unknowns.

4. Conclusions

The theory of deformation determination among different observation epochs has been reviewed. For the case of relative deformation networks it has been argued that the classical standard procedure, which is based on the use of the pseudoinverse matrix, has an implicit assumption that leads to consider among the infinitely many possible solutions one that attributes displacements to the majority of points. As it is claimed, this solution may not be representative of the expected scenario for many deformation monitoring networks. After having set a general framework for the study of particular solutions, the hypothesis of maximum number of stable points has been selected and developed. A final application illustrates how, as expected, the standard procedure fails in detecting the existing deformation whereas the maximum number of stable points procedure succeeds in the determination of place, direction and size of displacement for the cases were the stability of the great majority of the network points has to be incorporated as the most realistic hypothesis.

Appendix

For the rank-deficient system of consistent equations $Bx = b$, whose infinitely many solutions can be given by $x = B^{+}b + \left(I - B^{+}B\right)y$ with $y \in \Re^{n}$, the so-called pseudoinverse solution is obtained with $y = 0$, $x_p = B^{+}b$. We demonstrate here that the pseudoinverse solution is the minimum L_2-norm solution.

Let us start by showing that x_p and $\left(x - x_p\right)$ are orthogonal

$$x_p{}^{T}\left(x - x_p\right) = \left(B^{+}b\right)^{T}\left(x - B^{+}b\right) = \left(B^{+}BB^{+}b\right)^{T}\left(x - B^{+}b\right) \tag{25}$$

where we have made use of Eq. (14) $B^{+}BB^{+} = B^{+}$ in the first factor of the last equality. We can write the transpose of the matrix product in the right-hand member as $\left(B^{+}b\right)^{T}\left(B^{+}B\right)^{T}$ and take into account, Eq. (16), that $B^{+}B$ is symmetric. It follows that

$$x_p{}^{T}\left(x - x_p\right) = \left(B^{+}b\right)^{T}\left(B^{+}B\right)\left(x - B^{+}b\right) = \left(B^{+}b\right)^{T}\left(B^{+}Bx - B^{+}BB^{+}b\right) = \left(B^{+}b\right)^{T}\left(B^{+}Bx - B^{+}b\right) \tag{26}$$

where we have made use again of Eq. (14) $B^{+}BB^{+} = B^{+}$. Since $Bx = b$ we obtain, as we wanted to demonstrate, that

$$x_p{}^T\left(x - x_p\right) = \left(B^+ b\right)^T \left(B^+ b - B^+ b\right) = \left(B^+ b\right)^T .0 = 0 \tag{27}$$

From the trivial equality

$$x = x_p + \left(x - x_p\right) \tag{28}$$

we compute the L_2-norm squared on both sides

$$\left\|x\right\|_2^2 = \left\|x_p\right\|_2^2 + \left\|x - x_p\right\|_2^2 + 2x_p{}^T\left(x - x_p\right) \tag{29}$$

Since we have demonstrated that the last term is zero we obtain

$$\left\|x\right\|_2^2 = \left\|x_p\right\|_2^2 + \left\|x - x_p\right\|_2^2 \tag{30}$$

that is $\left\|x\right\|_2^2 \geq \left\|x_p\right\|_2^2$ with the equal sign if and only if $x = x_p$ as we wanted to demonstrate.

Acknowledgments The authors are grateful to the Editor and an anonymous reviewer for their valuable suggestions and constructive comments. This research is funded by the Spanish Ministry of Science and Innovation (AYA2011-23232).

References

[1] Kaloop MR, Li H (2014) Multi input-single output models identification of tower bridge movements using GPS monitoring system, *Measurement* 47: 531-539.

[2] Yi TH, Li HN, Gu M (2013) Experimental assessment of high-rate GPS receivers for deformation monitoring of bridge, *Measurement* 46: 420-432.

[3] Elnabwy MT, Kaloop MR, Elbeltagi E (2013) Talkha steel highway bridge monitoring and movement identification using RTK-GPS technique, *Measurement* 46: 4282-4292.

[4] Zheng S, Ma D, Zhang Z, Hu H, Gui L (2012) A novel measurement method based on silhouette for chimney quasi-static deformation monitoring, *Measurement* 45: 226-234.

[5] Pingue F, Petrazzuoli SM, Obrizzo F, Tammaro U, De Martino P, Zuccaro G (2011) Monitoring system of buildings with high vulnerability in presence of slow ground deformations (The Campi Flegrei, Italy, case), *Measurement* 44: 1628-1644.

[6] Xiao Z, Liang J, Yu D, Asundi A (2011) Large field-of-view deformation measurement for transmission tower based on close-range photogrammetry, *Measurement* 44: 1705-1712.

[7] Denli HH, Deniz R (2003) Global congruency test methods for GPS networks, *J. Surv. Eng* 129(3): 95-98.

[8] Yi TH, Li HN, Gu M (2013) Recent research and applications of GPS-based monitoring technology for high-rise structures, *Struct. Control. Health Monit.* 20: 649-670.

[9] Yi TH, Li HN, Gu M (2013) Wavelet based multi-step filtering method for bridge health monitoring using GPS and accelerometer, *Smart. Struct. Syst.* 11(4): 331-348.

[10] Yi TH, Li HN, Gu M (2011) Characterization and extraction of global positioning system multipath signals using an improved particle-filtering algorithm, *Meas. Sci. Technol.* 22: 075101 (11pp).

[11] Bernstein DS (2009) Matrix mathematics: theory, facts and formulas, 2nd Ed., Princeton University, Princeton, NJ.

[12] Sillard P, Boucher C (2001) A review of algebraic constraints in terrestrial reference frame datum definition, *J. Geod.* 75: 63-73.

[13] Xu P (1997) A general solution in geodetic non-linear rank defect models, *Boll Geod Sci Aff* 1: 1-25.

[14] Baselga S (2007) Global Optimization Solution of Robust Estimation, *J. Surv. Eng* 133(3): 123-128.

[15] Maronna RA, Martin RD, Yohai VJ (2006) Robust Statistics: Theory and Methods, Wiley, New York.

[16] Harvey BR (1993) Survey network adjustments by the L1 method, *Aust. J. Geod., Photogramm. Surv.* 59: 39–52.

[17] Baselga S, García-Asenjo L (2008) Global robust estimation and its application to GPS positioning, *Comput. Math. Appl*. 56: 709-714.

[18] Pardalos PM Romeijn HE (eds) (2002) Handbook of global optimization, Volume II, Kluwer Academic, Dordrecht.

[19] Holland JH (1975) Adaptation in natural and artificial systems, The University of Michigan Press, Ann Arbor, Mich.

[20] Zhou GD, Yi TH, Li HN (2014) Wireless sensor placement for bridge health monitoring using a generalized genetic algorithm, *Int. J. Str. Stab. Dyn.* 14: 1440011 (21pp).

[21] Floudas CA (2000) Deterministic global optimization: theory, methods and applications, Kluwer Academic, Dordrecht.

[22] Zhao RQ, Tang WS (2008) Monkey algorithm for global numerical optimization, *J. Uncertain. Syst.* 2: 165-176.

[23] Yi TH, Li HN, Zhang XD (2012) A modified monkey algorithm for optimal sensor placement in structural health monitoring, *Smart Mater. Struct.* 21: 105033 (9pp).

[24] Xu PL (2002) A hybrid global optimization method: the one-dimensional case. *J. Comput. Appl. Math.* 147: 301–314.

[25] Niemeier W (1981) Statistical tests for detecting movements in repeatedly measured geodetic networks, *Tectonophys.* 71: 335-351.

[26] Jokela J, Häkli P (2006) Current research and development at the Nummela standard baseline, XXIII FIG Congress, Munich, Germany, October 8-13.

[27] Rüeger JM (1996) Electronic Distance Measurement, Springer.